

# Biomedical Applications of Graphene and Graphene Oxide

CHUL CHUNG,<sup>†</sup> YOUNG-KWAN KIM,<sup>†</sup> DOLLY SHIN,  
SOO-RYOON RYOO, BYUNG HEE HONG,<sup>\*</sup> AND DAL-HEE MIN<sup>\*</sup>  
*Department of Chemistry, College of Natural Sciences, Seoul National University,  
Seoul, Korea*

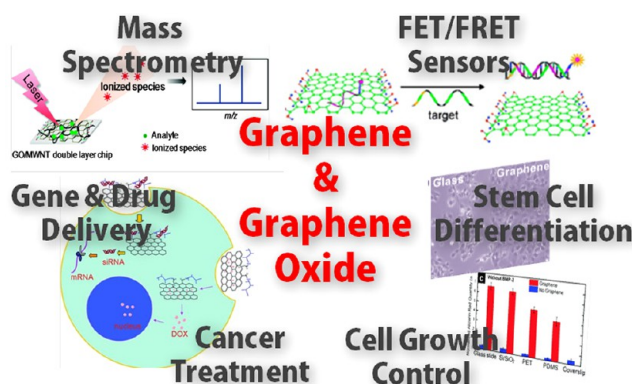
RECEIVED ON MAY 28, 2012

## CONSPECTUS

Graphene has unique mechanical, electronic, and optical properties, which researchers have used to develop novel electronic materials including transparent conductors and ultrafast transistors. Recently, the understanding of various chemical properties of graphene has facilitated its application in high-performance devices that generate and store energy. Graphene is now expanding its territory beyond electronic and chemical applications toward biomedical areas such as precise biosensing through graphene-quenched fluorescence, graphene-enhanced cell differentiation and growth, and graphene-assisted laser desorption/ionization for mass spectrometry. In this Account, we review recent efforts to apply graphene and graphene oxides (GO) to biomedical research and a few different approaches to prepare graphene materials designed for biomedical applications.

Because of its excellent aqueous processability, amphiphilicity, surface functionalizability, surface enhanced Raman scattering (SERS), and fluorescence quenching ability, GO chemically exfoliated from oxidized graphite is considered a promising material for biological applications. In addition, the hydrophobicity and flexibility of large-area graphene synthesized by chemical vapor deposition (CVD) allow this material to play an important role in cell growth and differentiation.

The lack of acceptable classification standards of graphene derivatives based on chemical and physical properties has hindered the biological application of graphene derivatives. The development of an efficient graphene-based biosensor requires stable biofunctionalization of graphene derivatives under physiological conditions with minimal loss of their unique properties. For the development graphene-based therapeutics, researchers will need to build on the standardization of graphene derivatives and study the biofunctionalization of graphene to clearly understand how cells respond to exposure to graphene derivatives. Although several challenging issues remain, initial promising results in these areas point toward significant potential for graphene derivatives in biomedical research.



## 1. Introduction

Carbon materials are known to be more environmentally and biologically friendly than inorganic materials, since the carbon is one of the most common elements in our ecosystem. In particular, graphite is a naturally occurring material that has been used in our daily lives for hundreds of years without critical toxicity issues. Thus, one can expect that graphene, a single layer of graphite,<sup>1–3</sup> would be also safe and useful for biological purposes. In the case of carbon nanotubes (CNTs) that do not exist naturally, their extreme one-dimensional

morphology is found to be rather cytotoxic. In comparison, the two-dimensional shape of graphene is expected to be negligibly harmful in mild concentration, so graphene materials would be readily applicable to biomedical research. Particularly, graphene oxide (GO) chemically exfoliated from oxidized graphite is considered as a promising materials for biological applications owing to its excellent aqueous processability, amphiphilicity, surface functionalizability, surface enhanced Raman scattering (SERS) property, and fluorescence quenching ability.

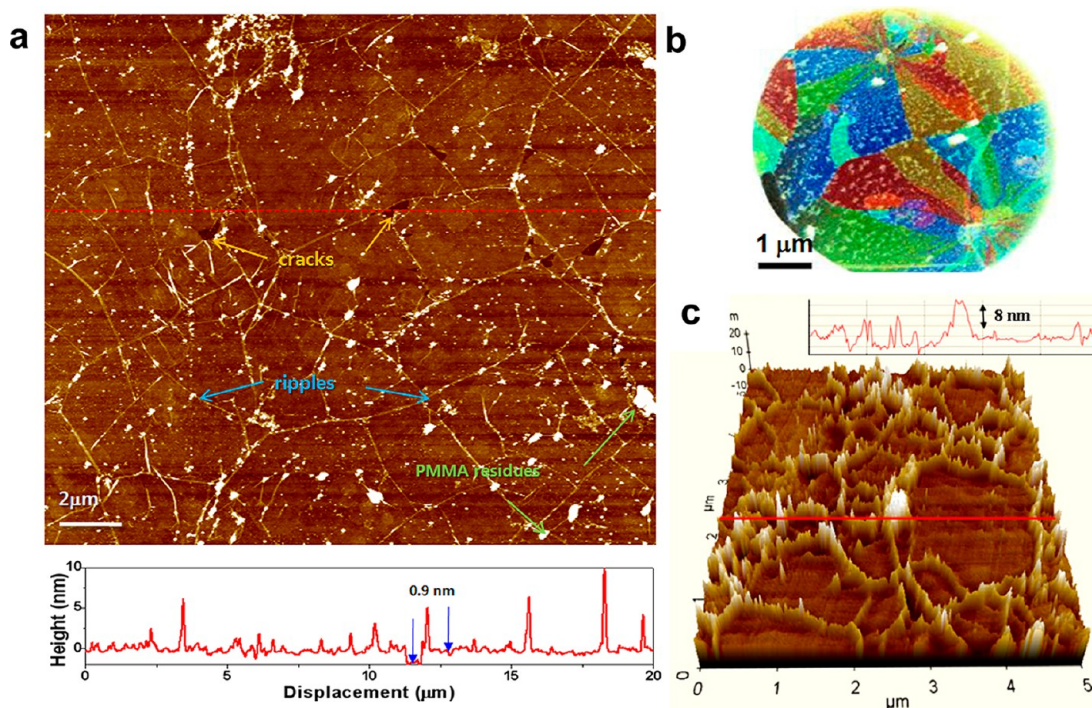


**FIGURE 1.** Nanoscale images showing the surface morphology of large-area graphene grown by CVD. (a) Atomic force microscope (AFM) image of a CVD graphene film transferred on a SiO<sub>2</sub> substrate. Adapted with permission from ref 10. Copyright 2010 Nature Publishing Group. (b) Transmission electron microscope image showing the polycrystalline domains of a CVD graphene film with false colors. Adapted from ref 13. Copyright 2011 Nature Publishing Group. (c) AMF image of electrodeposited CdSe quantum dots on CVD graphene, showing the higher electrochemical activity of grain boundaries or ripples. Adapted from ref 14. Copyright 2010 Wiley-VCH.

These fascinating properties of GOs are mainly derived from its unique chemical structures composed of small sp<sup>2</sup> carbon domains surrounded by sp<sup>3</sup> carbon domains and oxygen containing hydrophilic functional groups.<sup>4</sup> On the other hand, hydrophobicity and flexibility of large-area graphene synthesized by chemical vapor deposition (CVD) play an important role in cell growth and differentiation. Thus, it is of great importance to understand the characteristics of various graphene materials from different synthetic approaches before we discuss the actual application of graphene for biomedicine.

## 2. Synthesis of Graphene and GOs

**2.1. Large-Area Graphene Synthesized by CVD.** The mechanical exfoliation of graphite crystals by Scotch tape provides high quality graphene in microscale, but it is not compatible with large-scale synthesis for practical applications.<sup>2</sup> Alternative methods are chemical exfoliation of bulk graphite,<sup>5</sup> epitaxial graphene growth on SiC wafers,<sup>6</sup> gas-phase synthesis by CVD on Ni<sup>7</sup> or Cu,<sup>8</sup> and organic synthesis of graphene molecules.<sup>9</sup> Among these, the CVD synthesis has been most successful in producing larger scale and higher quality graphene films up to meter scale.<sup>10</sup>

Usually, the CVD reaction utilizes a catalytic reaction between hydrocarbon gases and catalytic metal substrates. More recent works also demonstrated the successful growth of graphene using solid sources such as polymethyl methacrylate (PMMA).<sup>11</sup> The first CVD growth of graphene was carried out on a Ni substrate.<sup>7</sup> The reaction is typically carried out at 1000 °C under low pressure to decompose the precursor gas into atomic radicals, which results in the dissolution of carbon atoms in Ni, followed by the segregation and crystallization of graphene during the cooling process. The mechanism of graphene growth on Cu is found to be different from the dissolution–segregation–crystallization on Ni. Since carbon solubility is close to zero on Cu, the carbon atoms are adsorbed and diffused on the surface of Cu, leading to the sequential formation of the hexagonal lattices.<sup>8</sup> Therefore, the larger single-crystalline graphene with controlled number of layers (mostly monolayers) can be achieved cost-effectively using commercially available Cu foils, which triggered the practical applications of graphene particularly for transparent conductors in large-area electronics.<sup>10</sup>

The CVD graphene synthesized at high-temperatures undergoes negative thermal expansion when it cools down to room temperature. Therefore, the graphene expands

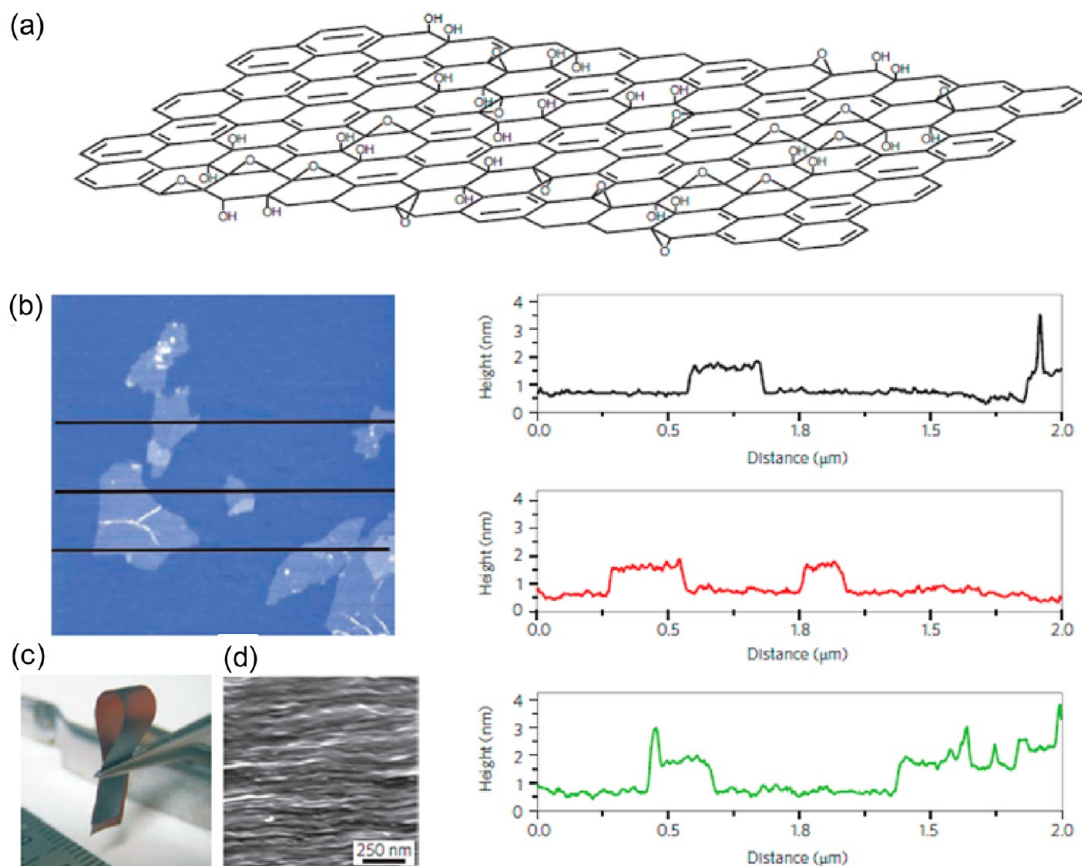


**FIGURE 2.** Chemical structure and nanoscale morphology of GO. (a) Chemical structure of graphene oxide. (b) AFM image and line profile of GO sheets with  $\sim 1$  nm thickness. (c, d) Photograph of folded GO paper and scanning electron microscope image of the cross-section of the GO paper. Adapted from ref 5. Copyright 2009 Nature Publishing Group.

laterally, while the metal substrate shrinks, which results in the formation of nanoscale ripples (Figure 1a).<sup>10</sup> Sometimes, the rough surface and step-edges of Cu leave sub-nanoripples, and these thermally or morphologically formed ripples considerably alter the electrical properties of graphene.<sup>12</sup> In addition, the CVD graphene show polycrystallinity as shown in Figure 1b, since the nucleated graphene domains are growing with random orientations.<sup>13</sup> Therefore, a lot of grain boundaries showing nonhexagonal carbon ring structures and vacancies are inevitably formed unlike highly oriented pyrolytic graphite (HOPG) surface. These defective structures including the ripples and the grain boundaries are found to be more chemically reactive,<sup>14</sup> which is an important factor to be considered when CVD graphene is used as a biological interface or platform.

**2.2. Graphene Oxides (GO).** The most widely used approach to GO synthesis is the Hummers method which involves oxidation of graphite by treatment with potassium permanganate ( $\text{KMnO}_4$ ) and sulfuric acid ( $\text{H}_2\text{SO}_4$ ).<sup>15</sup> The resulting graphite salts serve as precursors for GO by exfoliation in solvents with sonication. The chemical structure of GO is shown in Figure 2. GO can be converted into

graphene analogue by chemical and thermal reduction processes.<sup>5</sup> While the crystalline and electronic quality of graphene sheet made by GO is less than that of CVD graphene, in certain applications GO is preferred because of its simple transfer process (spin coated or sprayed on to virtually any substrates), easy scalability, and inexpensive synthesis. The unique chemical structure of GO also enables various chemical modification or functionalization useful for electrochemical or biomedical applications.

### 3. Graphene Field Effect Transistor (FET) Based Biosensors

The graphene FET has been extensively explored to develop sensitive chemical- and biosensors because of its functionalizable surface and highly sensitive electrical properties.<sup>16–23</sup> Detection of important biomolecules such as nucleic acids (NAs),<sup>16</sup> proteins,<sup>17,18</sup> and growth factors<sup>19</sup> have been successfully demonstrated by using appropriately functionalized graphene derivatives with NAs,<sup>16</sup> aptamers,<sup>17,19</sup> and carbohydrates<sup>18</sup> for monitoring target specific changes of electrical signal with high signal-to-noise ratio (Figure 3a).

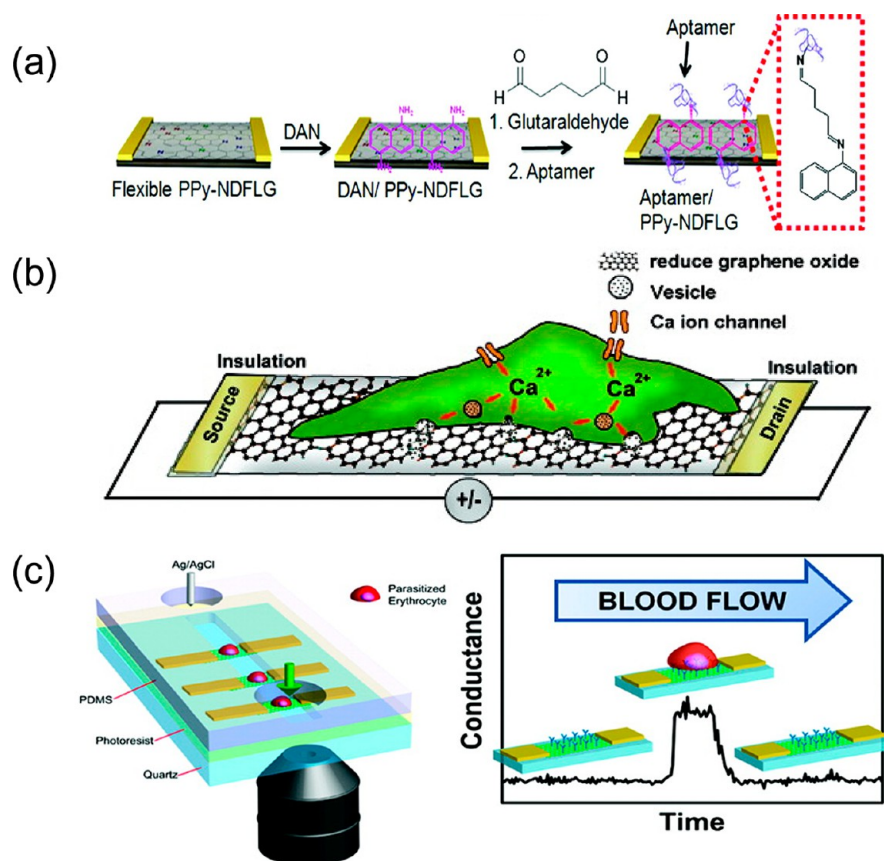


**FIGURE 3.** (a) Scheme of nitrogen doped graphene FET biosensor for detection of vascular endothelial growth factor (VEGF). Adapted with permission from ref 19. Copyright 2012 American Chemical Society. (b) CVD grown graphene FET biosensor for detection of hormonal catecholamine molecules. Adapted with permission from ref 20. Copyright 2010 American Chemical Society. (c) CVD grown graphene FET biosensor coupled with microchannel for detection of malaria infected RBCs. Adapted with permission from ref 21. Copyright 2011 American Chemical Society.

In addition to biomolecules in buffered solutions, hormonal catecholamine molecules secreted from living neuroendocrine PC12 cells have been also detected on poly-L-lysine functionalized RGO FET devices (Figure 3b).<sup>20</sup> Furthermore, a single malaria-infected red blood cell (RBC) has been also detected on the combined devices of microfluidic channel and arrays of FET devices fabricated on CVD graphene films which are functionalized with CD 36 receptor proteins (Figure 3c).<sup>21</sup>

The direct detection of biosignals from living cells on graphene FET devices was demonstrated based on the fact that graphene can form strongly coupled interface with cell membranes. The electrical signals from electrogenic cells, cardiomyocytes, have been successfully recorded on single<sup>22</sup> and array type<sup>23</sup> FET devices, respectively, fabricated on mechanically exfoliated graphene and CVD graphene with a high signal-to-noise ratio above 4, which exceeds typical values from other planar devices.

#### 4. GO FRET Biosensor

Many GO-based biosensing platforms rely on GO's preferential interaction with single-strand DNA (ssDNA) over

double-strand DNA (dsDNA). While the exposed nucleobases in ssDNA adsorb strongly with GO surface, nucleobases in dsDNA are effectively hidden in helical structure, which prevents the direct interaction of nucleobases with GO surface. Therefore, when fluorescently labeled ssDNA probes bound to the GO surface are hybridized with its complementary target ssDNA and detached from GO by forming a DNA duplex, the fluorescence that was quenched by GO gets recovered (Figure 4a).<sup>24</sup> Based on this concept, the detection of multiple ssDNA<sup>25</sup> and microribonucleic acid (microRNA) was successfully demonstrated. The limit of detection (LOD) was further improved by cyclic enzymatic amplification. (Figure 4b).<sup>26</sup> Recently, GO-organic dye ionic-complex was developed to detect dsDNA through ionic exchange on the carboxylic acid groups at the edges of GO.<sup>27</sup>

The target species for GO-based sensors have been extended to protein (Figure 4c),<sup>28</sup> hormone,<sup>29</sup> adenosine-5'-triphosphate (ATP),<sup>30</sup> and fungi toxin<sup>31</sup> with the use of GO-aptamer complexes. In addition to biomolecules, harmful metal ions such as Hg(II),<sup>32</sup> Ag(I),<sup>33</sup> Cu(II),<sup>34</sup> and Pb(II)<sup>35</sup> can

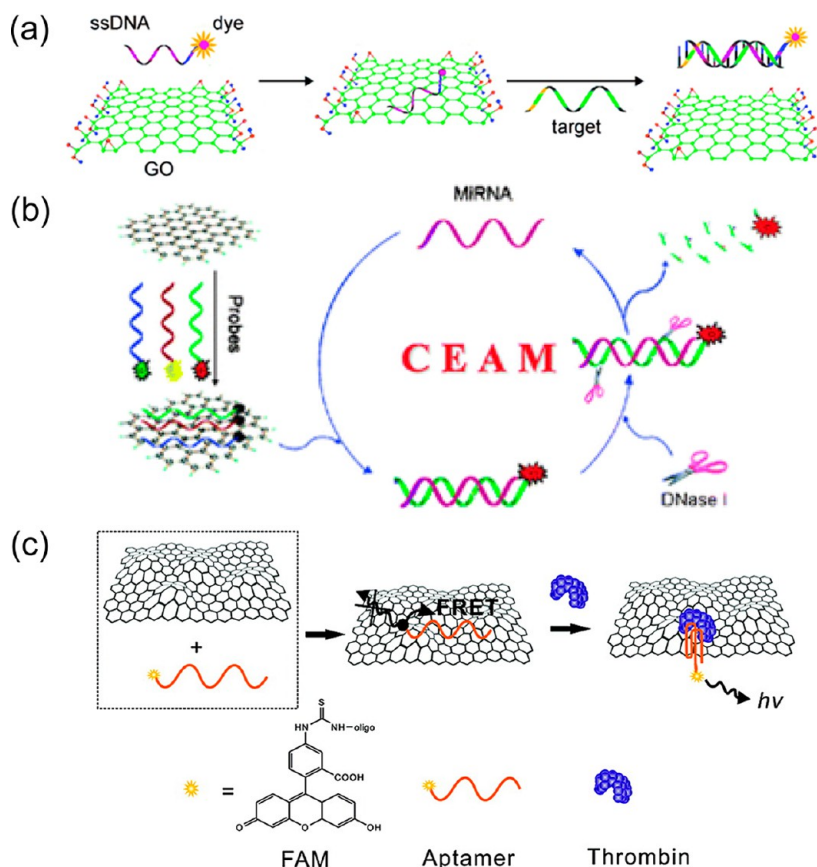


**FIGURE 4.** (a) Scheme of GO based sensor for ssDNA detection. Adapted from ref 24. (b) Multiple microRNA detection with signal amplification by cyclic enzyme reaction. Adapted from ref 26. (c) Thrombin detection. Adapted with permission from ref 28. Copyright 2010 American Chemical Society.

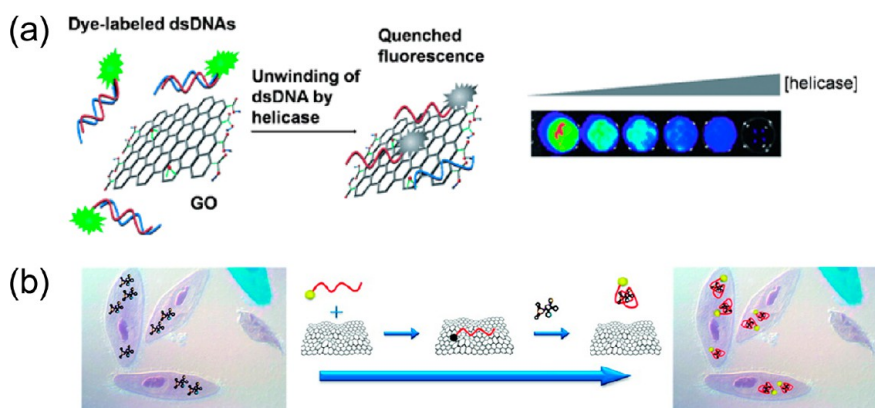


**FIGURE 5.** (a) Scheme of GO based system for DNA unwinding helicase activity assay. Adapted from ref 36. (b) ATP detection in live cells. Adapted from ref 44. Copyright 2010 American Chemical Society.

be detected by using GO complexes with fluorescent dye, cystein-rich ssDNA, or combination of ssDNAs and DNazymes.

Recently, the GO sensor has been applied to real-time duplex-unwinding helicase activity assay. The sensor monitors fluorescence quenching induced by helicase unwinding reaction of dsDNA, which contains fluorescent dye at the

end of one strand. The reaction results in binding of unwound ssDNA to GO and subsequent fluorescence quenching (Figure 5a).<sup>36</sup> After the development of this system, there has been many attempts to develop enzyme assay systems for DNA dependent protein kinase,<sup>37</sup> endonuclease/methyl transferase,<sup>38</sup> exonuclease,<sup>39</sup> and telomerase,<sup>40</sup> all of which

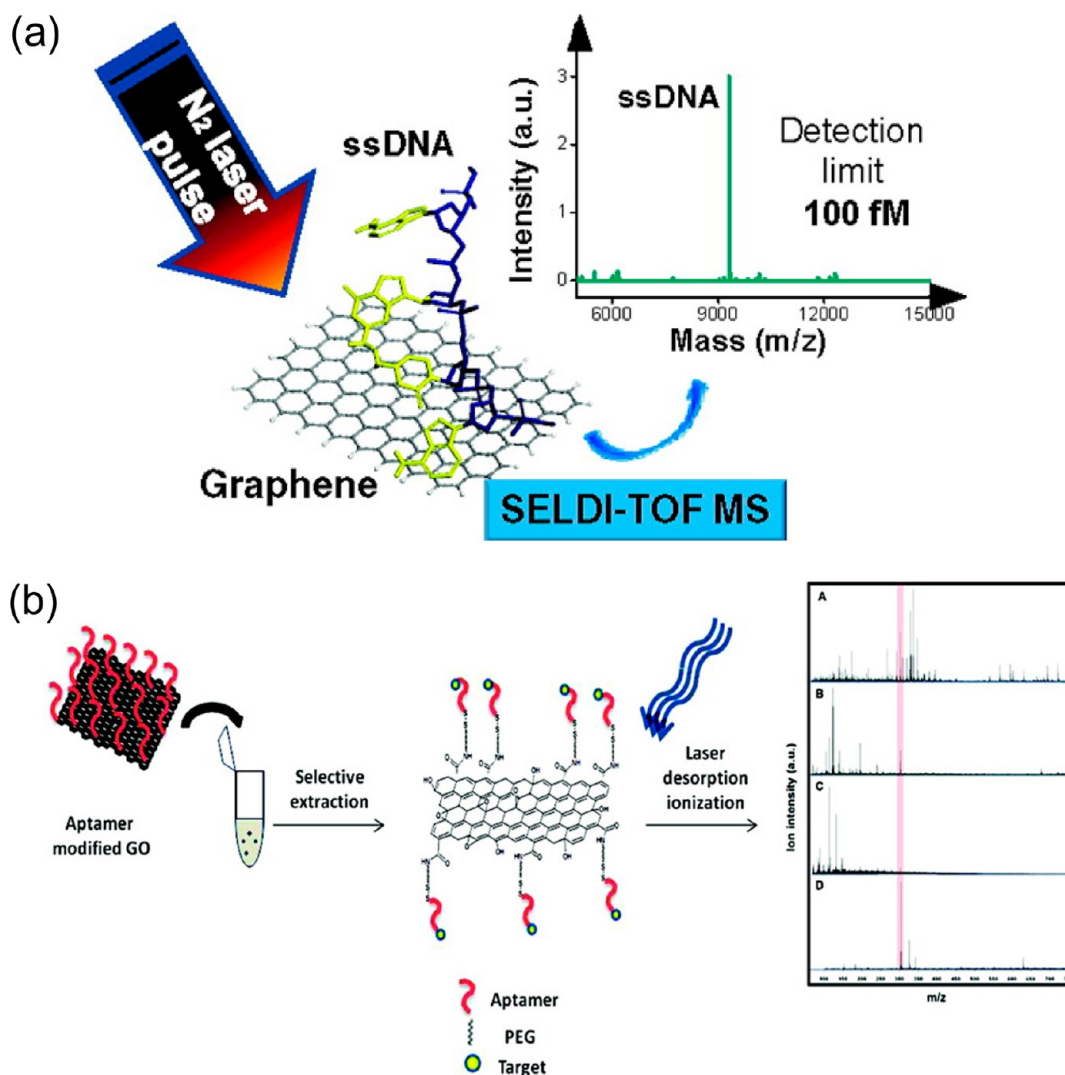


**FIGURE 6.** (a) Scheme of GO based mass spectrometric analysis for ssDNA and protein. Adapted with permission from ref 49. Copyright 2010 American Chemical Society. (b) Specific target by using aptamer conjugation. Adapted with permission from ref 52. Copyright 2010 American Chemical Society.

catalyze the biological reaction of NAs. By using fluorescent dye labeled peptides as probes, activities of several important proteases, such as trypsin,<sup>41</sup> thrombin,<sup>42</sup> and metalloproteinase-2,<sup>43</sup> were successfully monitored by protease-induced cleavage at specific sites of the peptide probes, resulting in fluorescence recovery.

In addition, GO biosensing platforms have been applied to live cells to detect ATP by using fluorescent dye labeled aptamer (Figure 5b)<sup>44</sup> and microRNA along with molecular beacon of locked nucleic acid.<sup>45</sup> Caspase-3 activity was also monitored in live cells by using GO that is covalently conjugated with fluorescent dye labeled substrate peptide.<sup>46</sup>

To increase efficiency of GO FRET biosensors, it is important to understand the molecular mechanism of the GO FRET and physical/chemical parameters related to the performance

of the sensors. In this regard, several reports are available which investigated relationship of the degree of GO reduction<sup>47</sup> and the length of fluorescently labeled ssDNA from GO<sup>48</sup> with fluorescence quenching capability.

## 5. GO LDI-MS Applications

Graphene derivatives have been considered as efficient matrices which can replace conventional organic matrices for LDI-MS because they effectively absorb and transfer UV-laser energy to analytes. The efficiency of graphene as a LDI-MS matrix was higher than that of GO and RGO due to the high heat dissipation and electron transfer properties.<sup>49</sup> Moreover, the hydrophobic surfaces make it affinity probe for LDI-MS analysis of trace amount of analytes, which have aromatic structures, including small molecules,<sup>50</sup> pollutant,<sup>51</sup> ssDNA and proteins (Figure 6a).<sup>49</sup>

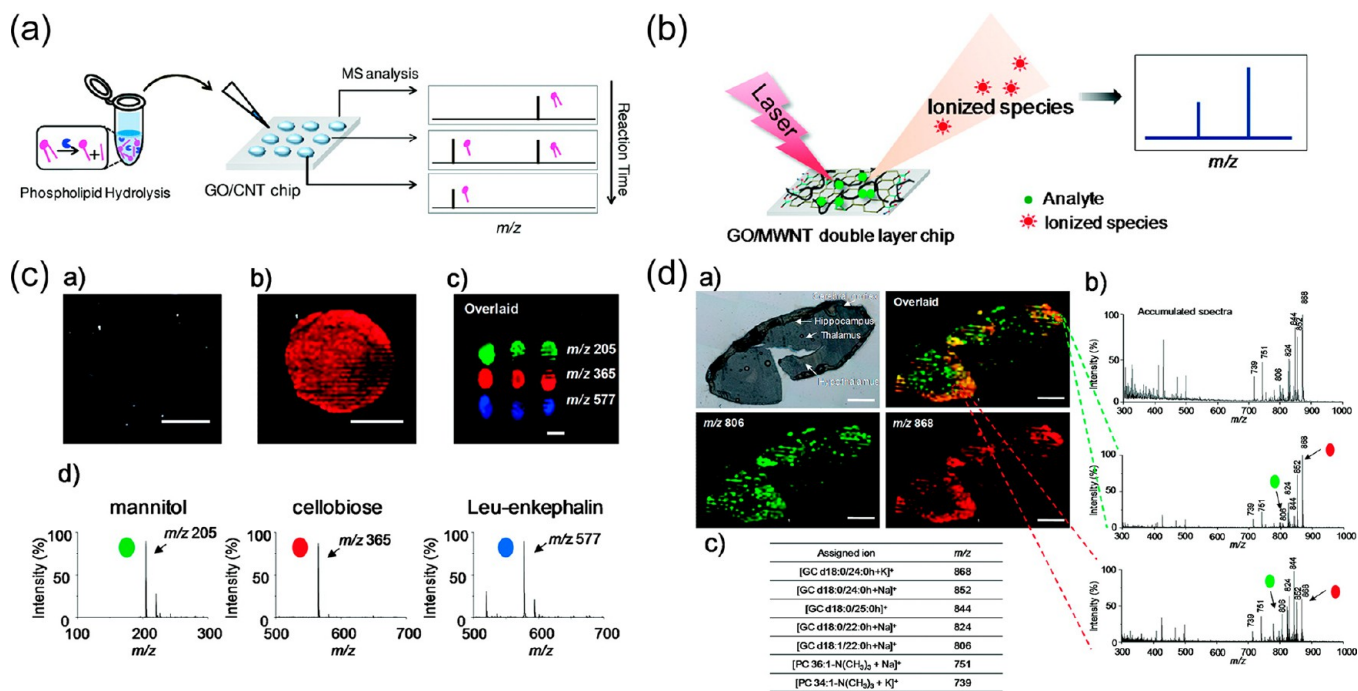


**FIGURE 7.** Application of GOs for biological mass spectrometry. (a) Scheme of GO/MWCNT films based mass spectrometric analysis for lipase activity assay. Adapted with permission from ref 57. Copyright 2010 American Chemical Society. (b) Scheme of LDI-MS application of GO/MWCNT films. (c, d) Scheme of mass spectrometric images of small molecules and mouse brain tissue on RGO/MWCNT films. Adapted from ref 58. Copyright 2011 American Chemical Society.

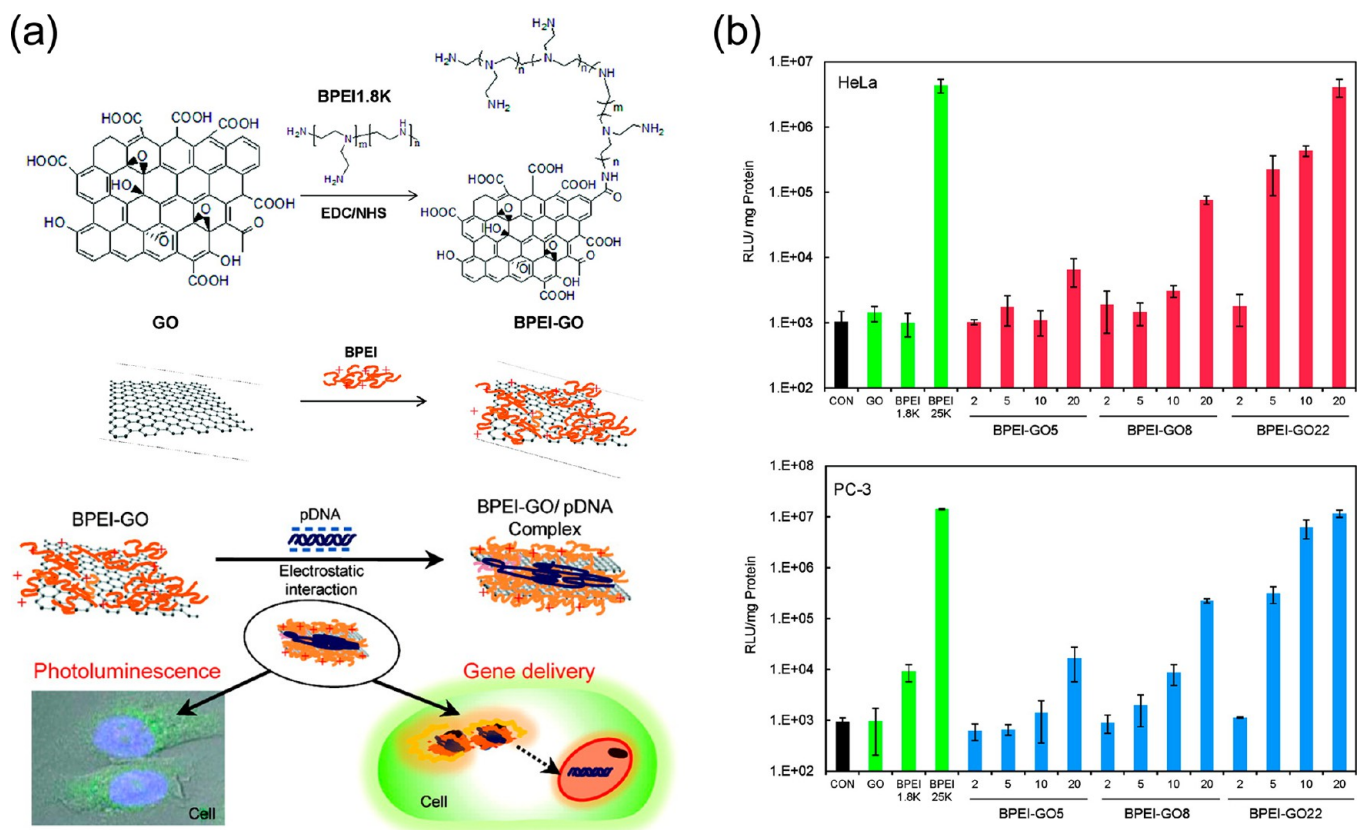


**FIGURE 8.** (a) Schemes of bPEI-GO complex with electrostatically adsorbed pDNA and covalently conjugated bPEI-GO. (b) Enhanced photoluminescence by pDNA loading on bPEI-GO. Adapted with permission from ref 62. Copyright 2011 American Chemical Society.

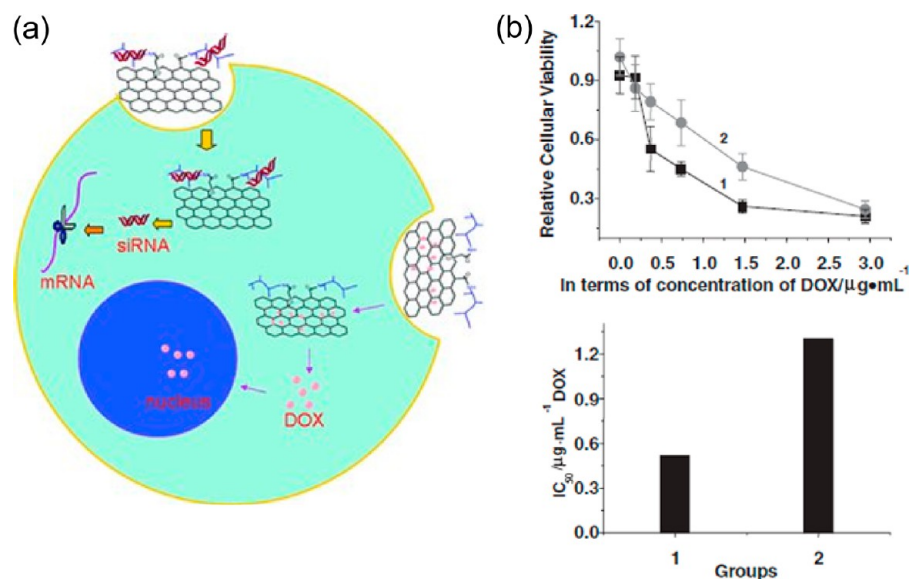


**FIGURE 9.** (a) Scheme of sequential delivery siRNA and DOX by using PEI-GO. (b) Target specific cell viability changing as function of dose of doxorubicin and  $\text{IC}_{50}$  value after pretreatment of siRNA-loaded PEI-GO complex (1, Bcl-2 siRNA; 2, scrambled siRNA). Adapted with permission from ref 63. Copyright 2011 Wiley-VCH.

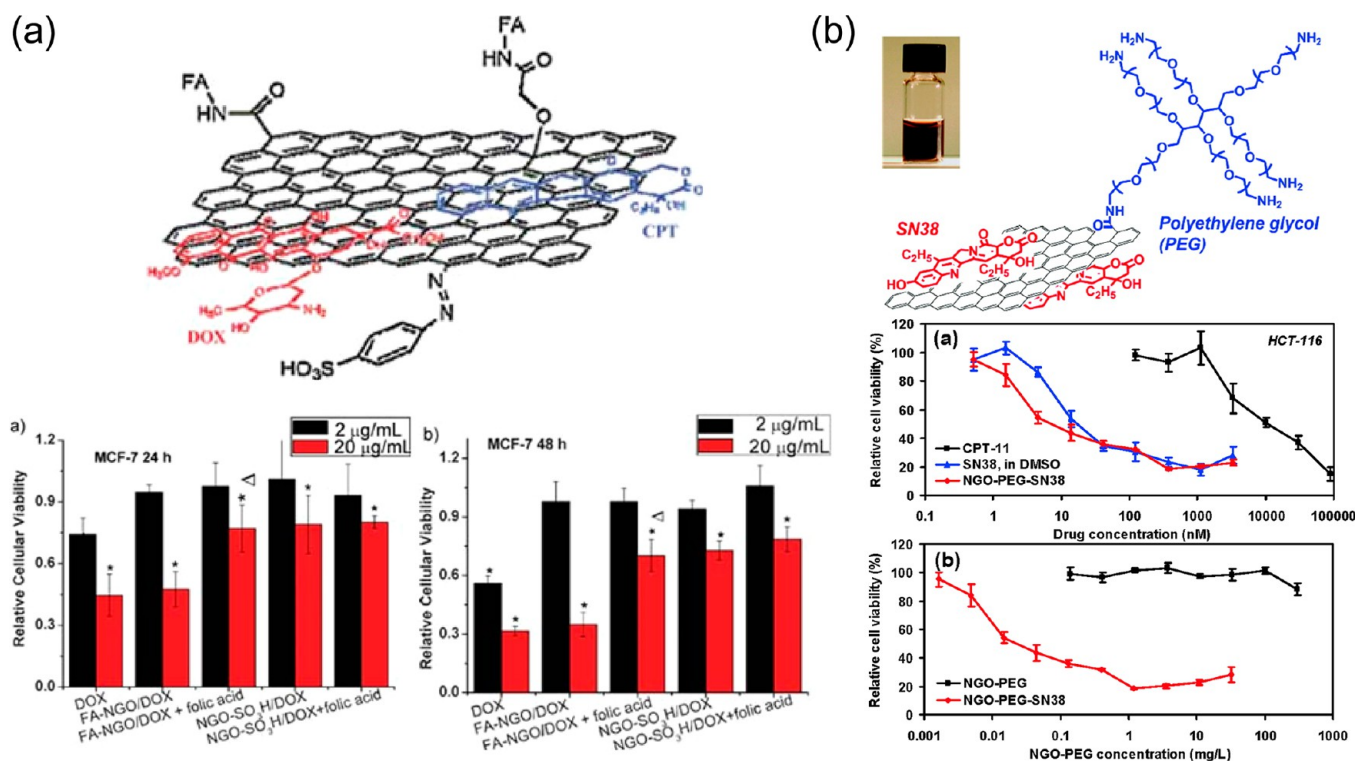


**FIGURE 10.** (a) FA-NGO loaded with two anticancer drugs for targeted and enhanced treatment of cancer cells. Adapted from ref 66. (b) SN-38 loaded NGO-PEG complex showing high cytotoxicity to HCT-116 cancer cells compared to control groups. Adapted with permission from ref 68. Copyright 2008 American Chemical Society.

By conjugating aptamers to GO, GO served as specific affinity probes and LDI substrate as well for target analytes (Figure 6b).<sup>52</sup> In addition, GO can be utilized as a support for synthesis of nanocomposites with  $\text{Fe}_3\text{O}_4$  for enrichment of

antibiotics by magnetic separation,<sup>53</sup> or with  $\text{TiO}_2$  for selective binding of phosphorylated biomolecules.<sup>54</sup>

Furthermore, GO-based nanohybrid films have been developed to enhance LDI efficiency by immobilization



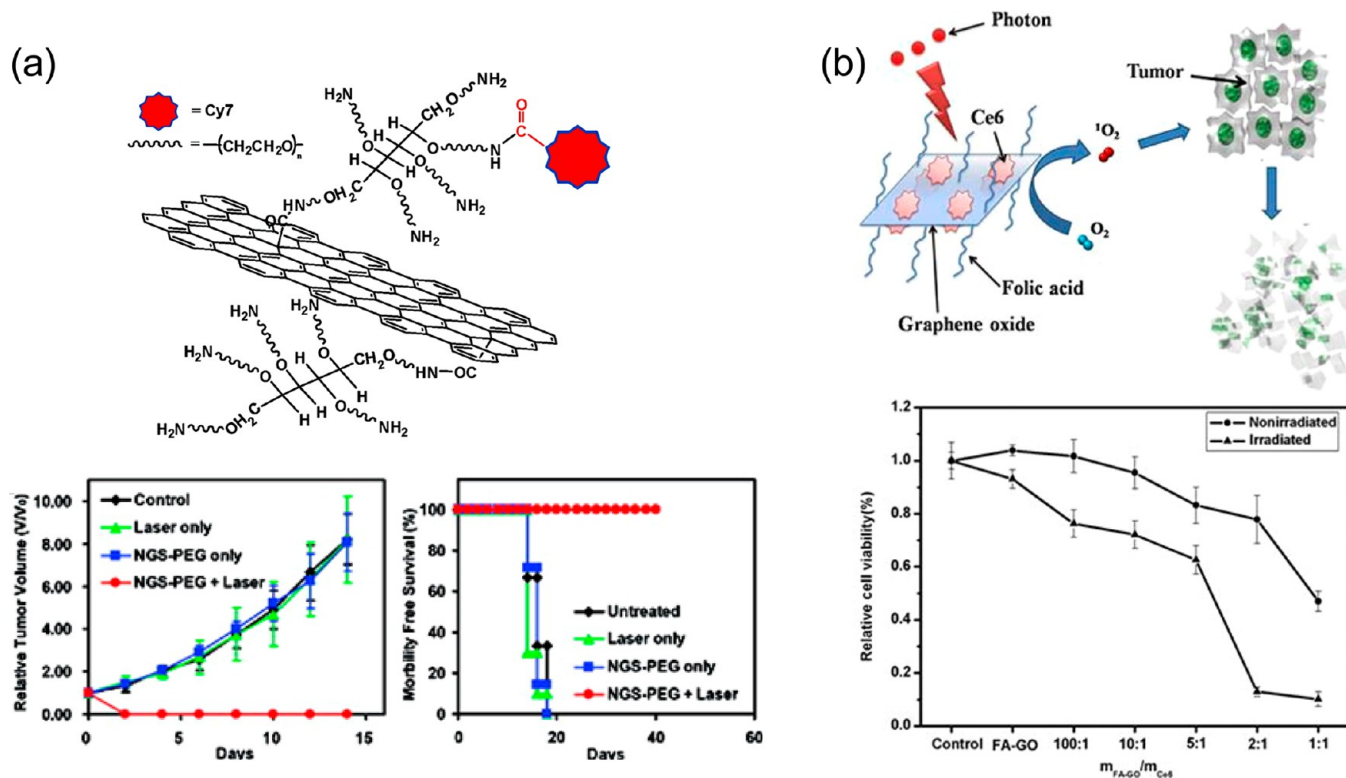


**FIGURE 11.** (a) Schematic diagram of Cy7-PEG-NGS and its photothermal activity for effective decrease of the tumor volumes and increase of the survival rates. Adapted with permission from ref 70. Copyright 2010 American Chemical Society. (b) Scheme of Ce6-loaded FA-GO and its high photodynamic efficacy to kill MGC803 cancer cells. Adapted from ref 73.

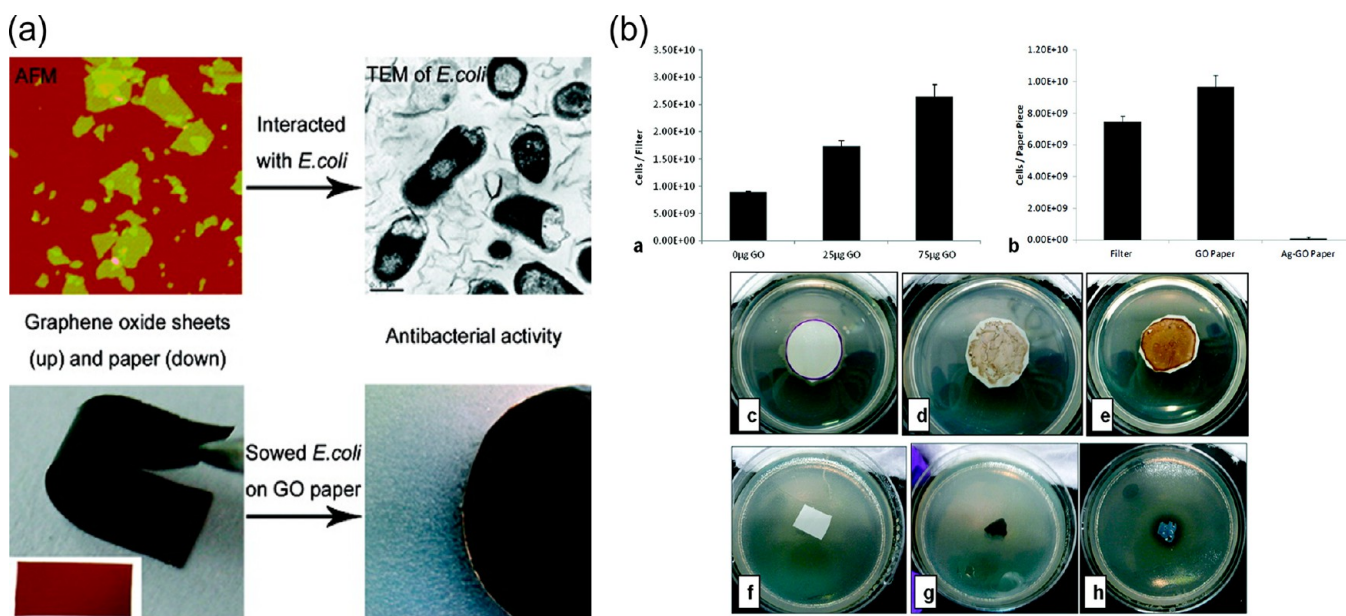


**FIGURE 12.** (a) Inhibition of *E. coli* growth on GO and RGO. Adapted with permission from ref 75. Copyright 2010 American Chemical Society. (b) Enhancement of *E. coli* growth on GO and RGO. Adapted with permission from ref 78. Copyright 2011 American Chemical Society.

of GO on a solid substrate and subsequent incorporation of multiwall carbon nanotubes (MWCNTs)<sup>55</sup> and gold nanostructures.<sup>56</sup> The GO/MWCNT films showed excellent

applicability for LDI-MS analysis of phospholipase activity (Figure 7a),<sup>57</sup> small molecules and mouse brain tissue (Figure 7b–d).<sup>58</sup> The LDI-MS efficiency of GO/MWCNT

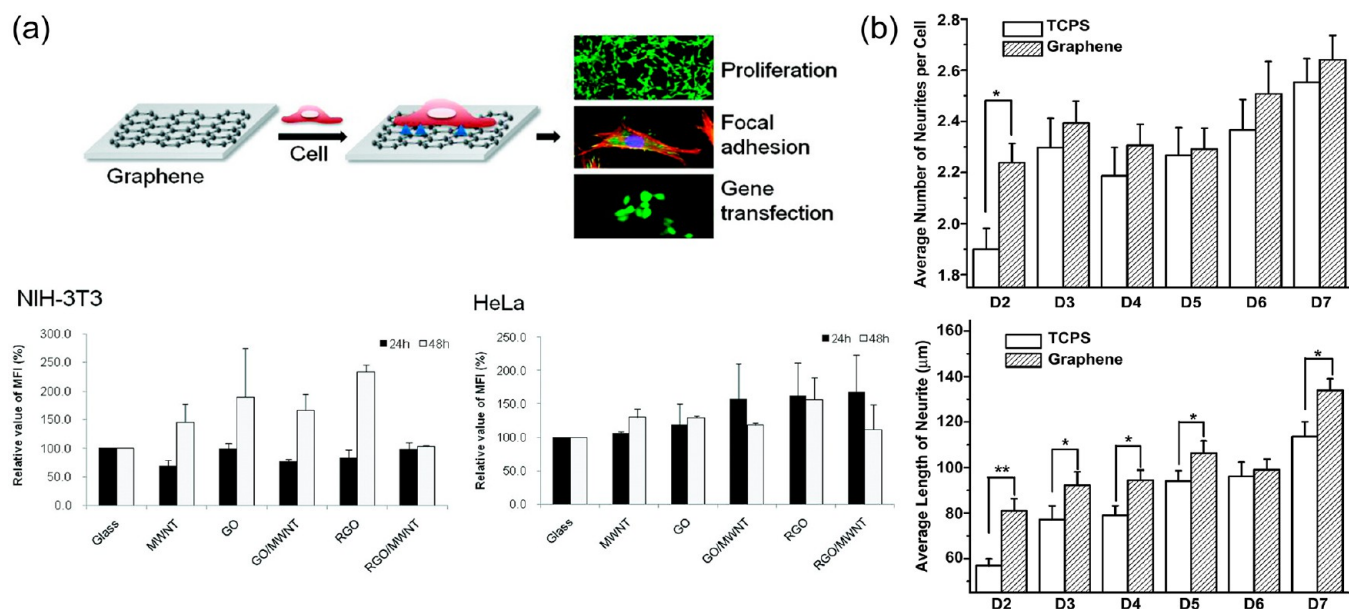


**FIGURE 13.** (a) Scheme of cellular behavior studies on carbon nanomaterials coated substrates with the enhanced gene transfection. Adapted with permission from ref 79. Copyright 2010 American Chemical Society. (b) Diagrams showing promoted neurite sprouting and outgrowth on graphene surface compared to tissue culture polystyrene. Adapted from ref 81.

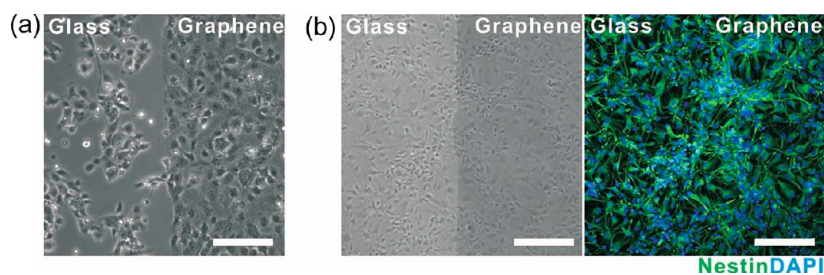


**FIGURE 14.** Bright-field image of hNSCs on the boundary area between glass and graphene 10 h after cell seeding (a). Bright-field (left) and fluorescence (right) images of hNSCs proliferated for 5 days showing no difference in the number of cells (b). All scale bars represent 200 μm.<sup>82</sup>

platform could be further improved by increasing the surface roughness and thickness.<sup>59</sup>

## 6. Graphene Derivatives as Delivery Carriers

**6.1. Gene Delivery.** Polyethyleneimine (PEI) has been extensively utilized as a surface modifier of GO sheets for gene delivery into cells by complexation through electrostatic interaction<sup>60</sup> and covalent conjugation for loading of plasmid DNA (pDNA). The covalent GO conjugates with linear<sup>61</sup> and branched PEI<sup>62</sup> showed high gene transfection efficiency with low cytotoxicity compared to PEI/pDNA complexes (Figure 8). Sequential delivery of Bcl-2 targeted siRNA and doxorubicin (DOX) into HeLa cells was also successfully demonstrated by using PEI-GO complex with the enhanced therapeutic efficacy (Figure 9).<sup>63</sup> Recently, chitosan-functionalized GO (CS-GO) complex was synthesized and

applied to efficient codelivery of anticancer drug and pDNA loaded respectively by  $\pi$ - $\pi$  and electrostatic interactions.<sup>64</sup>

**6.2. Small Molecule Drug Delivery.** Small molecule drugs having pH-dependent solubility have been widely used for pH-responsive delivery by using GO as a carrier. For example, DOX-GO complexes showed pH-responsive release of DOX from GO due to higher solubility of DOX at low pH condition.<sup>65</sup> Taking this advantage, pH-responsive codelivery of DOX and captothecin (CPT) was successfully demonstrated by using folic acid conjugated-nanoGO (FA-NGO) for cancer targeting (Figure 10a).<sup>66</sup> Anti-inflammatory drugs with different hydrophilicity (ibuprofen and 5-fluorouracil) were also delivered by using CS-GO complex with pH-responsive release.<sup>67</sup>

**6.3. Therapeutic Modalities for Cancer Treatment.** For efficient delivery of hydrophobic drugs, NGO have been functionalized with six-arm polyethyleneglycol (6-arm PEG)

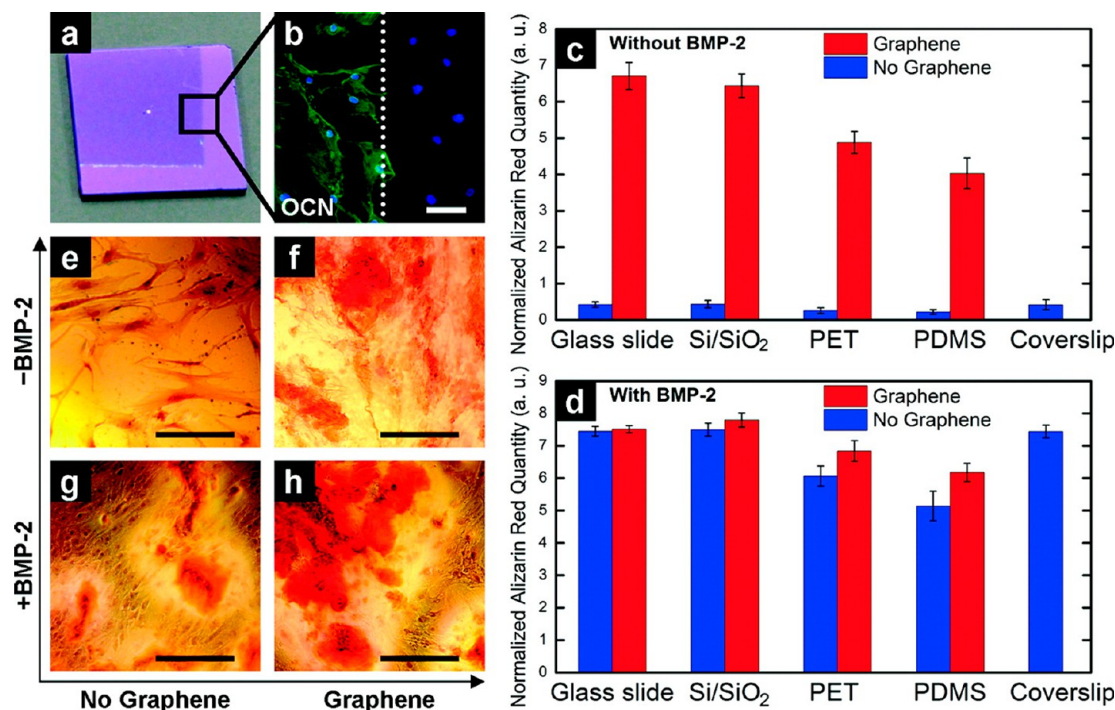


**FIGURE 15.** Optical image of partially graphene-coated Si/SiO<sub>2</sub> substrate (a). Osteocalcin (OCN) marker showing preferential bone cell formation on the graphene-coated area (b). Alizarin red quantification deriving from hMSCs grown for 15 days with/without BMP-2 on substrates with/without graphene (c,d). hMSCs grown on PET substrate under different conditions (BMP-2 and graphene coating) showing different osteogenic differentiation behavior confirmed by alizarin red staining (e–h). All scale bars are 100  $\mu\text{m}$ .<sup>83</sup>

and successfully applied to cancer cell lines with high cellular uptake and therapeutic efficacy (Figure 10b).<sup>68,69</sup> In addition to applications as a carrier, NGO derivatives have been utilized for photothermal therapy based on their high absorption of near-IR (NIR). High therapeutic efficacy of PEG-GO conjugate was demonstrated in mouse cancer xenograft models (Figure 11a).<sup>70</sup> Recently, it was reported that the phototherapeutic effect of NGO derivatives is originated from induction of the oxidative stress, mitochondrial depolarization, and caspase activation resulting in apoptotic and necrotic cell death.<sup>71</sup>

For enhancement of therapeutic efficacy by combinational therapy, PEG-GO has been used as a carrier for DOX for the combination of photothermal and chemical therapy.<sup>72</sup> Porphyrin photosensitizer has also been loaded on folic acid conjugated PEG-GO for combination of photothermal and photodynamic therapy with cancer targeting ability (Figure 11b).<sup>73</sup> In addition to the small molecule drugs, graphene/TiO<sub>2</sub> nanohybrid composite also showed high therapeutic efficacy based on the photothermal and photocatalytic therapy.<sup>74</sup>

## 7. Cell Growth Behavior on Graphene Surfaces

**7.1. Substrates for Antibacterial Effects.** The GO and RGO papers showed inhibition effect of bacterial growth

on their surfaces (Figure 12a).<sup>75</sup> The inhibition effect was demonstrated on GO and RGO nanowalls with both Gram-positive and Gram-negative bacteria. The antibacterial effect of RGO nanowalls was higher than that of GO nanowalls because of more efficient charge transfer of RGO with bacterial cells.<sup>76</sup> The antibacterial effect of graphene derivatives was derived from oxidative stress induced by membrane disruption.<sup>77</sup> On the other hand, one report suggested that bacterial growth was enhanced, rather than inhibited, on graphene surface (Figure 12b).<sup>78</sup> The controversial results indicated that the bacterial growth on GO could be varied with experimental conditions.

**7.2. Scaffolds for Mammalian Cell Culture.** Graphene derivatives were utilized as a substrate for mammalian cell culture. For example, the behavior of NIH-3T3 fibroblasts was investigated on various carbon nanomaterial-coated substrates such as GO, RGO, and carbon nanotubes. The carbon nanomaterial-coated substrates showed high biocompatibility and enhanced gene transfection efficiency (Figure 13a).<sup>79</sup> Graphene/chitosan hybrid films also showed promising applicability to tissue engineering to repair and improve tissue functions.<sup>80</sup> Interestingly, the neurite sprouting and outgrowth were also promoted on graphene surface compared to conventional tissue culture plate made of polystyrene (Figure 13b).<sup>81</sup>

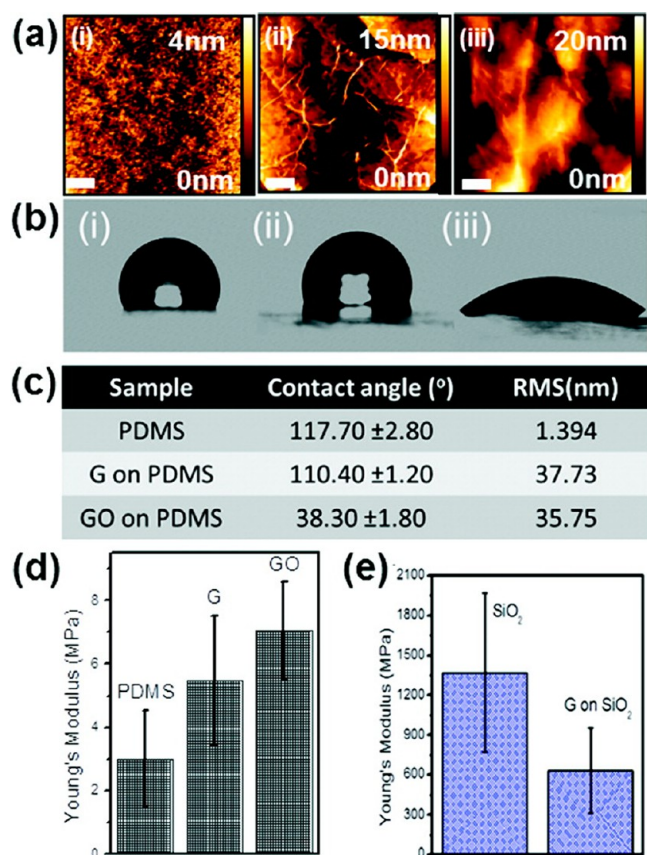


**FIGURE 16.** (a) AFM topography images of (i) PDMS, (ii) graphene (G) on PDMS, and (iii) GO on PDMS. (b) Contact angle images of (i) PDMS, (ii) G, and (iii) GO. (c) Table summarizing the contact angle and roughness (rms) of PDMS, G, and GO. (d) Young's modulus bar chart of PDMS, G, and GO. (e) Young's modulus bar chart of SiO<sub>2</sub> and G on SiO<sub>2</sub>. Inset: white scale bar indicates 1 μm length. Adapted with permission from ref 84. Copyright 2011 American Chemical Society.

**7.3. Differentiation of Stem Cells.** Stem cells are biologically important in living organisms because they can differentiate into any kinds of cell types for self-repair of organ and tissue by their continuous growth and renewal ontology. In regenerative medicine, the stem cells are considered as innovative therapeutic means, so-called stem cell therapy. Differentiation of stem cells into desired cell lines is one of the important research topics in stem cell study. Graphene was used for stem cell culture and differentiation mostly due to its biocompatibility and electrical conductivity.

Recently, the enhanced neuronal differentiation of human mesenchymal stem cells (hMSCs) was observed on graphene surface because graphene served as a cell-adhesion layer with electrical coupling effect for electrical stimulation for the differentiation (Figure 14).<sup>82</sup> In addition, graphene also enhanced the osteogenic differentiation comparable to common growth factor (Figure 15).<sup>83</sup> However, the mechanisms underlying differentiation are still not well understood. Graphene and

GO showed differences in inducing stem cell differentiation. One report indicated that the osteogenic differentiation was accelerated but adipogenic differentiation was suppressed on graphene compared to GO. The reason of distinct differentiation was the different interaction between growth agents and graphene and GO surfaces because of their different surface properties that can be controlled by various chemical functionalizations (Figure 16).<sup>84,85</sup>

## 8. Conclusion

The unique and fascinating properties of graphene derivatives such as functionalizable surfaces, strong UV absorption, SERS, and fluorescence and fluorescence quenching ability make them one of the most promising materials for biosensors, therapeutics, and tissue engineering as well as electronics. Although several challenging issues still remain, the biological applications of graphene derivatives have significant potential because many attempts have shown promising results regarding biofunctionalization and standardization of graphene derivatives by fractionation based on size, number of layers, and chemical functionalities. Furthermore, there are many unique advantages and still many chances to discover fascinating properties and potential applications. We expect that efforts with interdisciplinary approaches among chemistry, biology, and engineering will accelerate mechanistic understanding of graphene-based platforms for bioapplications and make current successful demonstrations more routinely implemented in diverse applications.

*This work was supported by the Global Research Lab (GRL) Program (2011-0021972), the Global Frontier Research Program (2011-0031627), the Research Center Program (EM1202) of IBS (Institute for Basic Science), and the Basic Science Research Program (2011-0017356, 2011K000615, 2011-0017587, 2009-0083540) through the National Research Foundation of Korea (NRF) funded by the Korean government (MEST).*

## BIOGRAPHICAL INFORMATION

**Chul Chung** received B. S. degree in Department of Chemistry at Korea University (Korea) in 2006 and Ph.D. degree in Department of Chemistry at Korea University (Korea) in 2012. He is currently a postdoctoral research associate of the Hong laboratory in Department of Chemistry at Seoul National University (Korea). His research interest is the synthesis of graphene quantum dots for biological applications.

**Young-Kwan Kim** received his B. S. degree in Department of Polymer Science and Engineering at Chungju National University (Korea) in 2008 and Ph.D. degree in Department of Chemistry at KAIST (Korea Advanced Institute of Science and Technology,

Korea) in 2012. He is currently a postdoctoral research associate of the Min laboratory in Department of Chemistry at Seoul National University (Korea). His research interest is the synthesis of graphene based nanohybrid structures for biological applications.

**Dolly Shin** received a B.S. degree in Earth and Environmental Engineering (EEE) at Columbia University in 2011. She worked as a research scientist in Prof. Hong's laboratory at Seoul National University. She is currently a graduate student (EEE) at Columbia University. Her research interest mainly focuses on the use of nanomaterials for environmental protection and recovery.

**Soo-Ryoon Ryoo** graduated in 2012 with a Ph.D. in the Department of Chemistry at the Korea Advanced Institute of Science and Technology (KAIST) and is now a Post-Doctoral Fellow in Prof. Min's laboratory at Seoul National University (SNU). Her work focuses on the development of drug delivery carriers and biosensing platforms based on various nanomaterials.

**Byung Hee Hong** received B.S. (1998), M.S. (2000), and Ph.D. (2002) degrees in chemistry from POSTECH (Korea). After spending 3.5 years as a postdoc at Columbia University (Advisor: Philip Kim), he joined the Department of Chemistry, Sungkyunkwan University as an assistant professor in 2007. Now he is an associate professor in the Department of Chemistry at Seoul National University. Prof. Hong developed a method of synthesizing large-scale graphene by chemical vapor deposition (CVD), which triggered chemical research toward the practical applications of graphene.

**Dal-Hee Min** received her Ph. D from University of Chicago (Prof. M. Mrksich) in 2005. She joined Prof. Sangeeta Bhatia's group as a postdoctoral researcher in Division of Health Science and Technology, MIT for two years. In Oct. 2007, she started her independent academic carrier at KAIST as an Assistant Professor of the Department of Chemistry and moved to Seoul National University (Korea) as an Associate Professor in 2011. Her group focuses particularly on the diverse biological applications of graphene derivatives and porous nanomaterials.

#### FOOTNOTES

\*To whom correspondence should be addressed. E-mail: byunghee@snu.ac.kr (B.H.H.); dalheemin@snu.ac.kr (D.H.M.).

The authors declare no competing financial interest.

†C.C. and Y.-K.K. contributed equally to this work.

#### REFERENCES

- Geim, A. K.; Novoselov, K. S. The rise of graphene. *Nat. Mater.* **2007**, *6*, 183–191.
- Novoselov, K. S.; Geim, A. K.; Morozov, S. V.; Jiang, D.; Zhang, Y.; Dubonos, S. V.; Grigorieva, I. V.; Firsov, A. A. Electric field effect in atomically thin carbon films. *Science* **2004**, *306*, 666–669.
- Zhu, Y.; Murali, S.; Cai, W.; Li, X.; Suk, J. W.; Potts, J. R.; Ruoff, R. S. Graphene and Graphene Oxide: Synthesis, Properties, and Applications. *Adv. Mater.* **2010**, *22*, 3906–3924.
- Loh, K. P.; Bao, Q.; Eda, G.; Chhowalla, M. Graphene oxide as a chemically tunable platform for optical applications. *Nat. Chem.* **2010**, *2*, 1015–1024.
- Park, S.; Rodney, S. R. Chemical methods for the production of graphenes. *Nat. Nanotechnol.* **2009**, *4*, 217–224.
- Berger, C.; Song, Z.; Li, T.; Li, X.; Ogbazghi, A. Y.; Feng, R.; Dai, Z.; Marchenkov, A. N.; Conrad, E. H.; First, P. N.; de Heer, W. A. Ultrathin epitaxial graphite: 2D electron gas properties and a route toward graphene-based nanoelectronics. *J. Phys. Chem. B* **2004**, *108*, 19912–19916.
- Kim, K. S.; Zhao, Y.; Jang, H.; Lee, S. Y.; Kim, J. M.; Kim, K. S.; Ahn, J.-H.; Kim, P.; Choi, J.-Y.; Hong, B. H. Large-Scale Pattern Growth of Graphene Films for Stretchable Transparent Electrodes. *Nature* **2009**, *457*, 706–710.
- Li, X. S.; Cai, W. W.; An, J.; Kim, S.; Nah, J.; Yang, D. X.; Piner, R.; Velamakanni, A.; Jung, I.; Tutuc, E.; et al. Large-Area Synthesis of High-Quality and Uniform Graphene Films on Copper Foils. *Science* **2009**, *324*, 1312–1314.
- Dössel, L.; Gherghel, L.; Feng, X.; Müllen, K. Graphene Nanoribbons by Chemists: Nanometer-Sized, Soluble, and Defect-Free. *Angew. Chem., Int. Ed.* **2011**, *50*, 2540–2543.
- Bae, S.; Kim, H.; Lee, Y.; Xu, X.; Park, J. S.; Zheng, Y.; Balakrishnan, J.; Lei, T.; Kim, H. R.; Song, Y. I.; Kim, Y. J.; Kim, K. S.; Ozyilmaz, B.; Ahn, J. H.; Hong, B. H.; Iijima, S. Roll-to-roll production of 30-in. graphene films for transparent electrodes. *Nat. Nanotechnol.* **2010**, *5*, 574–578.
- Sun, Z.; Yan, Z.; Yao, J.; Beitler, E.; Zhu, Y.; Tour, J. M. Growth of graphene from solid carbon sources. *Nature* **2010**, *468*, 549–552.
- Ni, G. X.; Zheng, Y.; Bae, S.; Kim, H. R.; Pachoud, A.; Kim, Y. S.; Tan, C. L.; Im, D.; Ahn, J. H.; Hong, B. H.; Ozyilmaz, B. Quasi-Periodic Nanoripples in Graphene Grown by Chemical Vapor Deposition and Its Impact on Charge Transport. *ACS Nano* **2012**, *6*, 1158–1164.
- Huang, P. Y.; Ruiz-Vargas, C. S.; van der Zande, A. M.; Whitney, W. S.; Levendorf, M. P.; Kevek, J. W.; Garg, S.; Alden, J. S.; Hustedt, C. J.; Zhu, Y.; Park, J.; McEuen, P. L.; Muller, D. A. Grains and grain boundaries in single-layer graphene atomic patchwork quilts. *Nature* **2011**, *469*, 389–392.
- Kim, Y.-T.; Han, J. H.; Hong, B. H.; Kwon, Y.-U. Electrochemical Synthesis of CdSe Quantum-Dot Arrays on a Graphene Basal Plane Using Mesoporous Silica Thin-Film Templates. *Adv. Mater.* **2010**, *22*, 515–518.
- Hummers, W. S.; Offeman, R. E. Preparation of graphitic oxide. *J. Am. Chem. Soc.* **1958**, *80*, 1339.
- Mohanty, N.; Berry, V. Graphene-based single-bacterium resolution biodevice and DNA transistor: interfacing graphene derivatives with nanoscale and microscale biocomponents. *Nano Lett.* **2008**, *8*, 4469–4476.
- Ohno, Y.; Maehashi, K.; Matsumoto, K. Label-free biosensors based on aptamer-modified graphene field-effect transistors. *J. Am. Chem. Soc.* **2010**, *132*, 18012–18013.
- Chen, Y.; Vedala, H.; Kotchey, G. P.; Audfray, A.; Cecioni, S.; Imbert, A.; Vidal, S.; Star, A. Electronic detection of lectins using carbohydrate-functionalized nanostructures: graphene versus carbon nanotubes. *ACS Nano* **2012**, *6*, 760–770.
- Kwon, O. S.; Park, S. J.; Hong, J. Y.; Han, A. R.; Lee, J. S.; Lee, J. S.; Oh, J. H.; Jang, J. Flexible FET-type VEGF aptasensor based on nitrogen-doped graphene converted from conducting polymer. *ACS Nano* **2012**, *6*, 1486–1493.
- He, Q.; Sudibya, H. G.; Yin, Z.; Wu, S.; Li, H.; Boey, F.; Huang, W.; Chen, P.; Zhang, H. Centimeter-long and large-scale micropatterns of reduced graphene oxide films: fabrication and sensing applications. *ACS Nano* **2010**, *4*, 3201–3208.
- Ang, P. K.; Li, A.; Jaiswal, M.; Wang, Y.; Hou, H. W.; Thong, J. T.; Lim, C. T.; Loh, K. P. Flow sensing of single cell by graphene transistor in a microfluidic channel. *Nano Lett.* **2011**, *11*, 5240–5246.
- Cohen-Kami, T.; Qing, Q.; Li, Q.; Fang, Y.; Lieber, C. M. Graphene and nanowire transistors for cellular interfaces and electrical recording. *Nano Lett.* **2010**, *10*, 1098–1102.
- Hess, L. H.; Jansen, M.; Maybeck, V.; Hauf, M. V.; Seifert, M.; Stutzmann, M.; Sharp, I. D.; Offenhäuser, A.; Garrido, J. A. Graphene transistor arrays for recording action potentials from electrogenic cells. *Adv. Mater.* **2011**, *23*, 5045–5049.
- Lu, C. H.; Yang, H. H.; Zhu, C. L.; Chen, X.; Chen, G. N. A graphene platform for sensing biomolecules. *Angew. Chem., Int. Ed.* **2009**, *48*, 4785–4787.
- He, S.; Song, B.; Li, D.; Zhu, C.; Qi, W.; Wen, Y.; Wang, L.; Song, S.; Fang, H.; Fan, C. A Graphene Nanoprobe for Rapid, Sensitive, and Multicolor Fluorescent DNA Analysis. *Adv. Funct. Mater.* **2010**, *20*, 453–459.
- Cui, L.; Lin, X.; Lin, N.; Song, Y.; Zhu, Z.; Chen, X.; Yang, C. J. Graphene oxide-protected DNA probes for multiplex microRNA analysis in complex biological samples based on a cyclic enzymatic amplification method. *Chem. Commun.* **2012**, *48*, 194–196.
- Balapanuru, J.; Yang, J. X.; Xiao, S.; Bao, Q.; Jahan, M.; Polavarapu, L.; Wei, J.; Xu, Q. H.; Loh, K. P. A graphene oxide-organic dye ionic complex with DNA-sensing and optical-limiting properties. *Angew. Chem., Int. Ed.* **2010**, *49*, 6549–6553.
- Chang, H.; Tang, L.; Wang, Y.; Jiang, J.; Li, J. Graphene fluorescence resonance energy transfer aptasensor for the thrombin detection. *Anal. Chem.* **2010**, *82*, 2341–2346.
- Pu, Y.; Zhu, Z.; Han, D.; Liu, H.; Liu, J.; Liao, J.; Zhang, K.; Tan, W. Insulin-binding aptamer-conjugated graphene oxide for insulin detection. *Analyst* **2011**, *136*, 4138–4140.
- He, Y.; Wang, Z. G.; Tang, H. W.; Pang, D. W. Low background signal platform for the detection of ATP: when a molecular aptamer beacon meets graphene oxide. *Biosens. Bioelectron.* **2011**, *29*, 76–81.
- Sheng, L.; Ren, J.; Miao, Y.; Wang, J.; Wang, E. PVP-coated graphene oxide for selective determination of ochratoxin A via quenching fluorescence of free aptamer. *Biosens. Bioelectron.* **2011**, *26*, 3494–3499.
- Huang, W. T.; Shi, Y.; Xie, W. Y.; Luo, H. Q.; Li, N. B. A reversible fluorescence nanoswitch based on bifunctional reduced graphene oxide: use for detection of Hg<sup>2+</sup> and molecular logic gate operation. *Chem. Commun.* **2011**, *47*, 7800–7802.
- Wen, Y.; Xing, F.; He, S.; Song, S.; Wang, L.; Long, Y.; Li, D.; Fan, C. A graphene-based fluorescent nanoprobe for silver(I) ions detection by using graphene oxide and a silver-specific oligonucleotide. *Chem. Commun.* **2010**, *46*, 2596–2598.

- 34 Liu, M.; Zhao, H.; Chen, S.; Yu, H.; Zhang, Y.; Quan, X. Label-free fluorescent detection of Cu(II) ions based on DNA cleavage-dependent graphene-quenched DNazymes. *Chem. Commun.* **2011**, *47*, 7749–7751.
- 35 Zhao, X. H.; Kong, R. M.; Zhang, X. B.; Meng, H. M.; Liu, W. N.; Tan, W.; Shen, G. L.; Yu, R. Q. Graphene-DNAzyme based biosensor for amplified fluorescence "turn-on" detection of Pb<sup>2+</sup> with a high selectivity. *Anal. Chem.* **2011**, *83*, 5062–5066.
- 36 Jang, H.; Kim, Y. K.; Kwon, H. M.; Yeo, W. S.; Kim, D. E.; Min, D. H. A graphene-based platform for the assay of duplex-DNA unwinding by helicase. *Angew. Chem., Int. Ed.* **2010**, *49*, 5703–5707.
- 37 Lin, L.; Liu, Y.; Zhao, X.; Li, J. Sensitive and rapid screening of T4 polynucleotide kinase activity and inhibition based on coupled exonuclease reaction and graphene oxide platform. *Anal. Chem.* **2011**, *83*, 8396–8402.
- 38 Lee, J.; Kim, Y. K.; Min, D. H. A new assay for endonuclease/methyltransferase activities based on graphene oxide. *Anal. Chem.* **2011**, *83*, 8906–8912.
- 39 Lee, J.; Min, D. H. A simple fluorometric assay for DNA exonuclease activity based on graphene oxide. *Analyst* **2012**, *137*, 2024–2026.
- 40 Peng, L.; Zhu, Z.; Chen, Y.; Han, D.; Tan, W. An exonuclease III and graphene oxide-aided assay for DNA detection. *Biosens. Bioelectron.* **2012**, *35*, 475–478.
- 41 Gu, X.; Yang, G.; Zhang, G.; Zhang, D.; Zhu, D. A new fluorescence turn-on assay for trypsin and inhibitor screening based on graphene oxide. *ACS Appl. Mater. Interfaces.* **2011**, *3*, 1175–1179.
- 42 Zhang, M.; Yin, B. C.; Wang, X. F.; Ye, B. C. Interaction of peptides with graphene oxide and its application for real-time monitoring of protease activity. *Chem. Commun.* **2011**, *47*, 2399–2401.
- 43 Feng, D.; Zhang, Y.; Feng, T.; Shi, W.; Li, X.; Ma, H. A graphene oxide-peptide fluorescence sensor tailor-made for simple and sensitive detection of matrix metalloproteinase 2. *Chem. Commun.* **2011**, *47*, 10680–10682.
- 44 Wang, Y.; Li, Z.; Hu, D.; Lin, C. T.; Li, J.; Lin, Y. Aptamer/graphene oxide nanocomplex for in situ molecular probing in living cells. *J. Am. Chem. Soc.* **2010**, *132*, 9274–9276.
- 45 Dong, H.; Ding, L.; Yan, F.; Ji, H.; Ju, H. The use of polyethylenimine-grafted graphene nanoribbon for cellular delivery of locked nucleic acid modified molecular beacon for recognition of microRNA. *Biomaterials* **2011**, *32*, 3875–3882.
- 46 Wang, H.; Zhang, Q.; Chu, X.; Chen, T.; Ge, J.; Yu, R. Graphene oxide-peptide conjugate as an intracellular protease sensor for caspase-3 activation imaging in live cells. *Angew. Chem., Int. Ed.* **2011**, *50*, 7065–7069.
- 47 Hong, B. J.; An, Z.; Compton, O. C.; Nguyen, S. T. Tunable Biomolecular Interaction and Fluorescence Quenching Ability of Graphene Oxide: Application to "Turn-on" DNA Sensing in Biological Media. *Small* **2012**, *8*, 2469–2476.
- 48 Huang, P. J.; Liu, J. DNA-length-dependent fluorescence signaling on graphene oxide surface. *Small* **2012**, *8*, 977–983.
- 49 Tang, L. A.; Wang, J.; Loh, K. P. Graphene-based SELDI probe with ultrahigh extraction and sensitivity for DNA oligomer. *J. Am. Chem. Soc.* **2010**, *132*, 10976–10977.
- 50 Dong, X.; Cheng, J.; Li, J.; Wang, Y. Graphene as a novel matrix for the analysis of small molecules by MALDI-TOF MS. *Anal. Chem.* **2010**, *82*, 6208–6214.
- 51 Zhou, X.; Wei, Y.; He, Q.; Boey, F.; Zhang, Q.; Zhang, H. Reduced graphene oxide films used as matrix of MALDI-TOF-MS for detection of octachlorodibenzo-p-dioxin. *Chem. Commun.* **2010**, *46*, 6974–6976.
- 52 Gulbakan, B.; Yasun, E.; Shukoor, M. I.; Zhu, Z.; You, M.; Tan, X.; Sanchez, H.; Powell, D. H.; Dai, H.; Tan, W. A Dual Platform for Selective Analyte enrichment and ionization in mass spectrometry using aptamer-conjugated graphene oxide. *J. Am. Chem. Soc.* **2010**, *132*, 17408–17410.
- 53 Luo, Y. B.; Shi, Z. G.; Gao, Q.; Feng, Y. Q. Magnetic retrieval of graphene: extraction of sulfonamide antibiotics from environmental water samples. *J. Chromatogr., A* **2011**, *1218*, 1353–1358.
- 54 Lu, J.; Wang, M.; Li, Y.; Deng, C. Facile synthesis of TiO<sub>2</sub>/graphene composites for selective enrichment of phosphopeptides. *Nanoscale* **2012**, *4*, 1577–1580.
- 55 Kim, Y. K.; Min, D. H. Durable large-area thin films of graphene/carbon nanotube double layers as a transparent electrode. *Langmuir* **2009**, *25*, 11302–11306.
- 56 Kim, Y. K.; Min, D. H. Preparation of the hybrid film of poly(allylamine hydrochloride)-functionalized graphene oxide and gold nanoparticle and its application for laser-induced desorption/ionization of small molecules. *Langmuir* **2012**, *28*, 4453–4458.
- 57 Lee, J.; Kim, Y. K.; Min, D. H. Laser desorption/ionization mass spectrometric assay for phospholipase activity based on graphene oxide/carbon nanotube double-layer films. *J. Am. Chem. Soc.* **2010**, *132*, 14714–14717.
- 58 Kim, Y. K.; Na, H. K.; Kwack, S. J.; Ryoo, S. R.; Lee, Y.; Hong, S.; Hong, S.; Jeong, Y.; Min, D. H. Synergistic effect of graphene oxide/MWCNT films in laser desorption/ionization mass spectrometry of small molecules and tissue imaging. *ACS Nano* **2011**, *5*, 4550–4561.
- 59 Kim, Y. K.; Min, D. H. Fabrication of alternating multilayer films of graphene oxide and carbon nanotube and its application in mechanistic study of laser desorption/ionization of small molecules. *ACS Appl. Mater. Interfaces* **2012**, *4*, 2088–2095.
- 60 Feng, L. Z.; Zhang, S.; Liu, Z. Graphene based gene transfection. *Nanoscale* **2011**, *3*, 1252–1257.
- 61 Chen, B.; Liu, M.; Zhang, L. M.; Huang, J.; Yao, J. L.; Zhang, Z. J. Polyethylenimine-functionalized graphene oxide as an efficient gene delivery vector. *J. Mater. Chem.* **2011**, *21*, 7736–7741.
- 62 Kim, H.; Nangung, R.; Singha, K.; Oh, I. K.; Kim, W. J. Graphene oxide-polyethylenimine nanoconstruct as a gene delivery vector and bioimaging tool. *Bioconjugate Chem.* **2011**, *22*, 2558–2567.
- 63 Zhang, L. M.; Lu, Z.; Zhao, Q.; Huang, J.; Shen, H.; Zhang, Z. Enhanced chemotherapy efficacy by sequential delivery of siRNA and anticancer drugs using PEI-grafted graphene oxide. *Small* **2011**, *7*, 460–464.
- 64 Bao, H. Q.; Pan, Y. Z.; Ping, Y.; Sahoo, N. G.; Wu, T.; Li, L.; Li, J.; Gan, L. H. Chitosan-functionalized graphene oxide as a nanocarrier for drug and gene delivery. *Small* **2011**, *7*, 1569–1578.
- 65 Yang, X. Y.; Zhang, X. Y.; Liu, Z. F.; Ma, Y. F.; Huang, Y.; Chen, Y. S. High-efficiency loading and controlled release of doxorubicin hydrochloride on graphene oxide. *J. Phys. Chem. C* **2008**, *112*, 17554–17558.
- 66 Zhang, L. M.; Xia, J.; Zhao, Q.; Liu, L.; Zhang, Z. Functional graphene oxide as a nanocarrier for controlled loading and targeted delivery of mixed anticancer drugs. *Small* **2010**, *6*, 537–544.
- 67 Rana, V. K.; Choi, M. C.; Kong, J. Y.; Kim, G. Y.; Kim, M. J.; Kim, S. H.; Mishra, S.; Singh, R. P.; Ha, C. S. Synthesis and drug-delivery behavior of chitosan-functionalized graphene oxide hybrid nanosheets. *Macromol. Mater. Eng.* **2011**, *296*, 131–140.
- 68 Liu, Z.; Robinson, J. T.; Sun, X.; Dai, H. PEGylated nanographene oxide for delivery of water-insoluble cancer drugs. *J. Am. Chem. Soc.* **2008**, *130*, 10876–10877.
- 69 Sun, X.; Liu, Z.; Welscher, K.; Robinson, J. T.; Goodwin, A.; Zoric, S.; Dai, H. Nano-Graphene Oxide for Cellular Imaging and Drug Delivery. *Nano Res.* **2008**, *1*, 203–212.
- 70 Yang, K.; Zhang, S.; Zhang, G. X.; Sun, X.; Lee, S. T.; Liu, Z. Graphene in mice: ultrahigh in vivo tumor uptake and efficient photothermal therapy. *Nano Lett.* **2010**, *10*, 3318–3323.
- 71 Markovic, Z. M.; Harhaji-Trajkovic, L. M.; Todorovic-Markovic, B. M.; Kević, D. P.; Arskic, K. M.; Jovanović, S. P.; Pantovic, A. C.; Dramićanin, M. D.; Trajkovic, V. S. In vitro comparison of the photothermal anticancer activity of graphene nanoparticles and carbon nanotubes. *Biomaterials* **2011**, *32*, 1121–1129.
- 72 Zhang, W.; Guo, Z. Y.; Huang, D. Q.; Liu, Z.; Guo, X.; Zhong, H. Synergistic effect of chemophotothermal therapy using PEGylated graphene oxide. *Biomaterials* **2011**, *32*, 8555–8561.
- 73 Huang, P.; Xu, C.; Lin, J.; Wang, C.; Wang, X.; Zhang, C.; Zhou, X.; Guo, S.; Cui, D. Folic acid-conjugated graphene oxide loaded with photosensitizers for targeting photodynamic therapy. *Theranostics* **2011**, *1*, 240–250.
- 74 Hu, Z.; Huang, Y. D.; Sun, S. F.; Guan, W. C.; Yao, Y. H.; Tang, P. Y.; Li, C. Y. Visible light driven photodynamic anticancer activity of graphene oxide/TiO<sub>2</sub> hybrid. *Carbon* **2012**, *50*, 994–1004.
- 75 Hu, W. B.; Peng, C.; Luo, W. J.; Lv, M.; Li, X.; Li, D.; Huang, Q.; Fan, C. Graphene-based antibacterial paper. *ACS Nano* **2010**, *4*, 4317–4323.
- 76 Akhavan, O.; Ghaderi, E. Toxicity of graphene and graphene oxide nanowalls against bacteria. *ACS Nano* **2010**, *4*, 5731–5736.
- 77 Liu, S. B.; Zeng, T. H.; Hofmann, M.; Burcombe, E.; Wei, J.; Jiang, R.; Kong, J.; Chen, Y. Antibacterial activity of graphite, graphite oxide, graphene oxide, and reduced graphene oxide: membrane and oxidative stress. *ACS Nano* **2011**, *5*, 6971–6980.
- 78 Ruiz, O. N.; Fernando, K. A.; Wang, B.; Brown, N. A.; Luo, P. G.; McNamara, N. D.; Vangness, M.; Sun, Y. P.; Bunker, C. E. Graphene oxide: a nonspecific enhancer of cellular growth. *ACS Nano* **2011**, *5*, 8100–8107.
- 79 Ryoo, S. R.; Kim, Y. K.; Kim, M. H.; Min, D. H. Behaviors of NIH-3T3 fibro-blasts on graphene/carbon nanotubes: Proliferation, focal adhesion, and gene transfection studies. *ACS Nano* **2010**, *4*, 6587–6598.
- 80 Fan, H. L.; Wang, L. L.; Zhao, K. K.; Li, N.; Shi, Z.; Ge, Z.; Jin, Z. Fabrication, mechanical properties, and biocompatibility of graphene-reinforced chitosan composites. *Biomacromolecules* **2010**, *11*, 2345–2351.
- 81 Li, N.; Zhang, X. M.; Song, Q.; Su, R.; Zhang, Q.; Kong, T.; Liu, L.; Jin, G.; Tang, M.; Cheng, G. The promotion of neurite sprouting and outgrowth of mouse hippocampal cells in culture by graphene substrates. *Biomaterials* **2011**, *32*, 9374–9382.
- 82 Park, S. Y.; Park, J.; Sim, S. H.; Sung, M. G.; Kim, K. S.; Hong, B. H.; Hong, S. Enhanced differentiation of human neural stem cells into neurons on graphene. *Adv. Mater.* **2011**, *23*, H263–267.
- 83 Nayak, T. R.; Andersen, H.; Makam, V. S.; Khaw, C.; Bae, S.; Xu, X.; Ee, P. L.; Ahn, J. H.; Hong, B. H.; Pastorin, G.; Ozylmaz, B. Graphene for controlled and accelerated osteogenic differentiation of human mesenchymal stem cells. *ACS Nano* **2011**, *5*, 4670–4678.
- 84 Lee, W. C.; Lim, C. H.; Shi, H.; Tang, L. A.; Wang, Y.; Lim, C. T.; Loh, K. P. Origin of enhanced stem cell growth and differentiation on graphene and graphene oxide. *ACS Nano* **2011**, *5*, 7334–7341.
- 85 Wang, Y.; Lee, W. C.; Manga, K. K.; Ang, P. K.; Lu, J.; Liu, Y. P.; Lim, C. T.; Loh, K. P. Fluorinated graphene for promoting neuro-induction of stem cells. *Adv. Mater.* **2012**, *24*, 4285–4290.